



# FAPEX: Fractional Amplitude-Phase Expressor for Robust Cross-Subject Seizure Prediction

Ruizhe Zheng<sup>1</sup> § , Lingyan Mao<sup>2</sup> § , Dingding Han<sup>3\*</sup>, Tian Luo<sup>4</sup>, Yi Wang<sup>4</sup>, Jing Ding<sup>2\*</sup>, Yuguo Yu<sup>1\*</sup>

<sup>1</sup> Research Institute of Intelligent Complex Systems, Fudan University<sup>2</sup> Department of Neurology, Zhongshan Hospital, Fudan University<sup>3</sup> School of Information Science and Technology, Fudan University<sup>4</sup> Children's Hospital of Fudan University

Correspondence: ddhan@fudan.edu.cn, jingding@zs-hospital.sh.cn, yuyuguo@fudan.edu.cn

§ These authors contributed equally.

# Background & Motivation

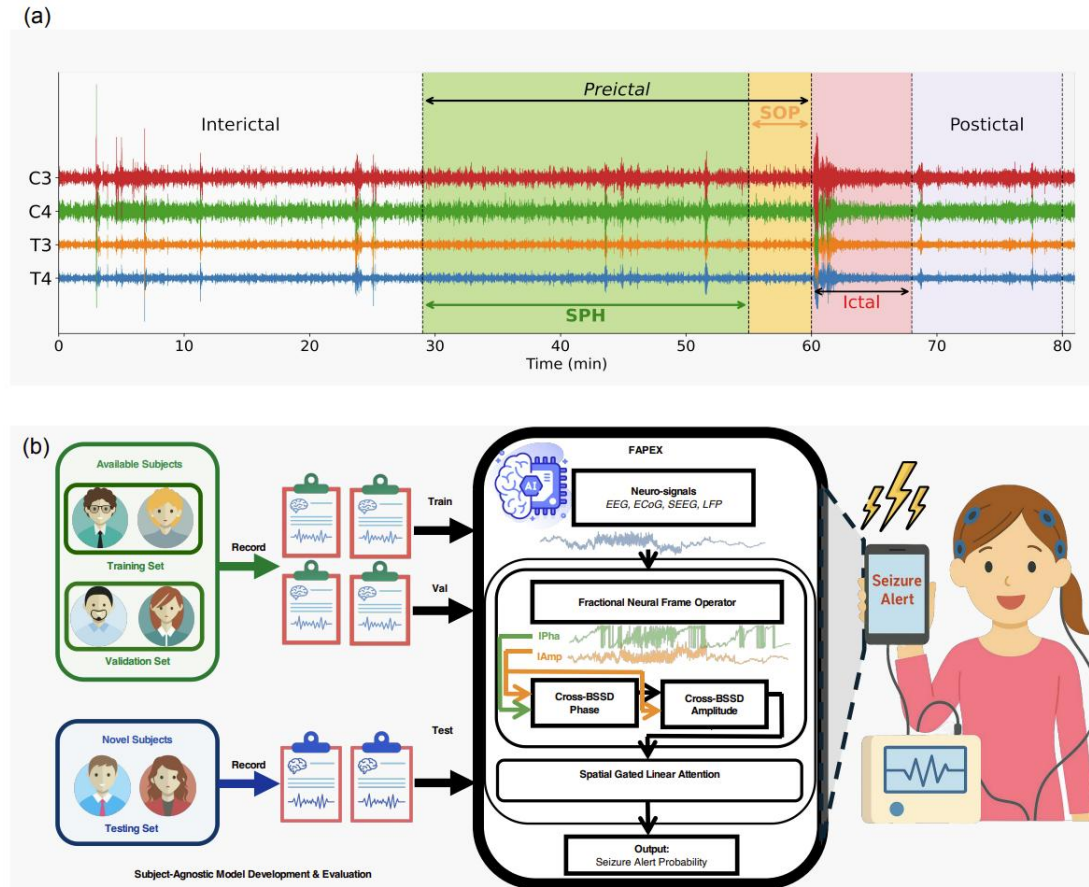
## Why is SASP Important?

### Clinical Practicality:

- New patients arriving at the hospital can use the model immediately
- No need to wait weeks to collect personal data
- Significantly reduces deployment costs

### Scientific Significance:

- Proves the existence of universal pre-seizure patterns
- Challenges the traditional notion that "every patient is unique"
- Provides a new perspective for understanding epilepsy mechanisms
- All of these can serve as major advantages—this paper



# Challenges

- 1. Preserve both high- and low-frequency biomarkers (HFOs & slow oscillations).
- 2. Model dynamic phase–amplitude coupling across frequencies.
- 3. Handle heterogeneous electrode layouts & variable channel numbers.

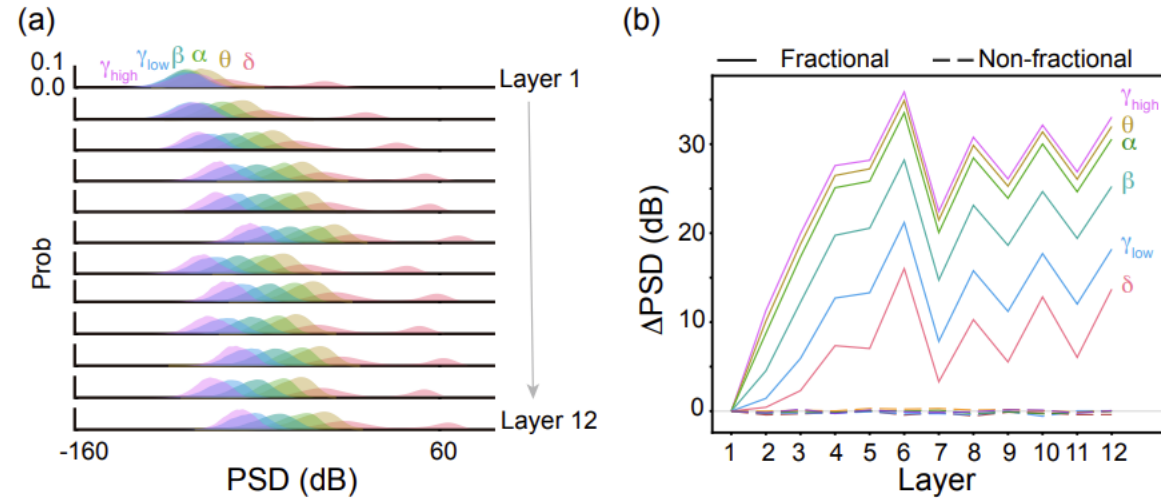


**Figure 2: Interpretability of FAPEX.** (a) Kernel density estimates of power spectral density (PSD) responses for FrNFO filters across layers and brain frequency subbands. As depth increases, the operator progressively refines its discrimination among subbands, maintaining the natural low-frequency, high-energy and high-frequency, low-energy distribution, with energy gradually stabilizing after intermediate layers. (b) Layer-wise frequency-specific gain relative to the initial layer. Unlike non-fractional operators, FrNFO consistently amplifies both low- and high-frequency components, achieving balanced cross-frequency representations, indicating its ability to capture both fast and slow neural dynamics essential for seizure prediction.

# FAPEX Framework Overview

- FrNFO: Fractional Neural Frame Operator – adaptive time–frequency decomposition.
- APCE: Amplitude–Phase Cross Encoding – bidirectional selective state-space modeling.
- SCA: Spatial Correlation Aggregation – channelwise linear attention.
- Unified training and evaluation via subject-agnostic nested cross-validation.

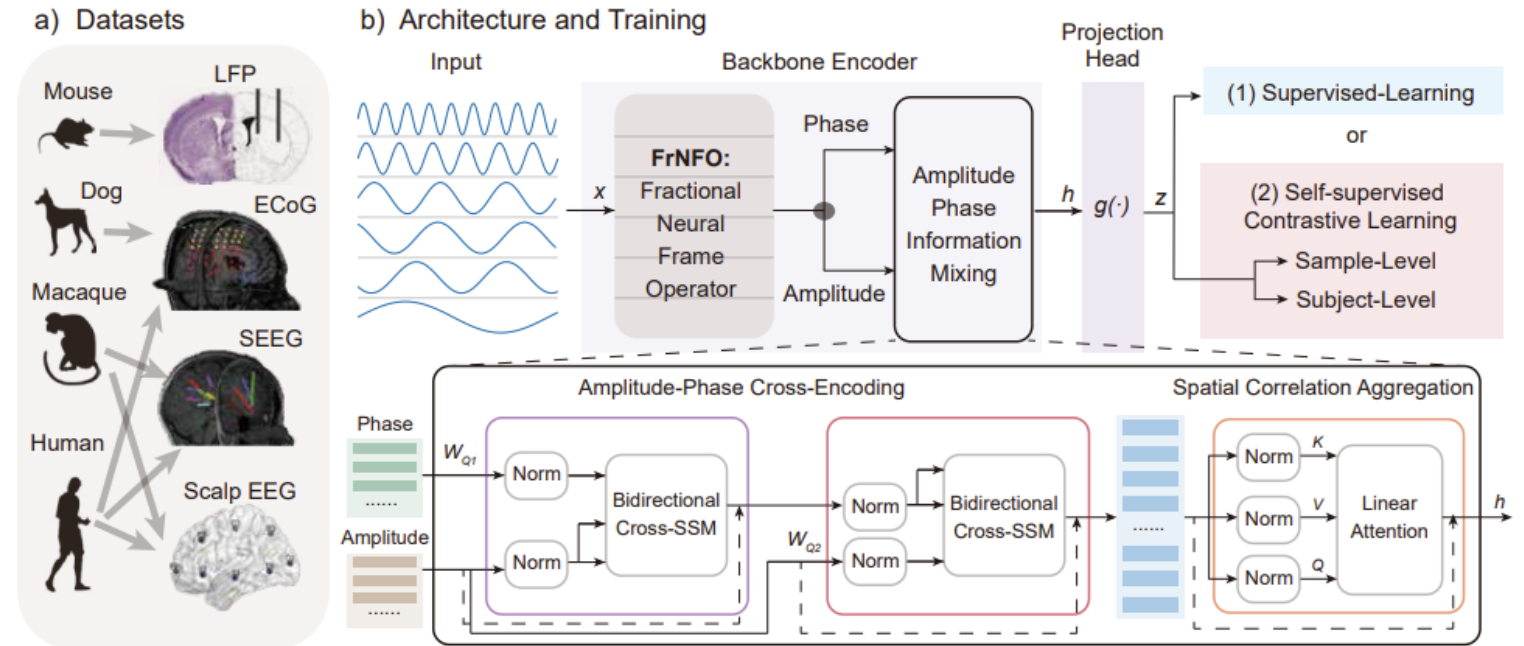


**Figure 3:** Datasets and network architecture summarization. (a) We used LFP, ECoG, SEEG and Scalp EEG data across species (humans, dogs, rats, and macaques), to validate our model. (b) The network structure and training pipeline of our FAPEX framework. The input signals will be encoded by the backbone encoder that is consisted of our FrNFO, naturally separated into phase and amplitude sections, then go through a Amplitude-Phase information mixing procedure which deals with the two sections interactively using 2 bidirectional Cross-SSM modules, and use a linear attention module for spatial correlation aggregation.



# FrNFO

- Learnable fractional-order convolutions with adaptive multi-scale windows.
- Each channel learns its fractional order  $\theta$  independently.
- Preserves high-frequency oscillations with minimal spectral leakage.
- Provably robust amplitude representation from a scattering perspective.

$$\Psi_\theta = \left\{ M_{lp_0^{(j)}}^\theta T_{sq_0^{(j)}}^\theta I\Phi_j : s \in \mathbb{R}, l \in \mathbb{Z}, j \in \{1, \dots, N\} \right\}, \quad (3)$$

where  $p_0^j, q_0^j$  are positive constants adjusting the scale. It involves  $\theta$ -modulation  $M_{lp_0^{(j)}}^\theta(t) = e^{\pi i((lp_0^{(j)})^2 \cot \theta + 2lp_0^{(j)}t \csc \theta)}$  and  $\theta$ -shift  $T_{sq_0^{(j)}}^\theta(t) = e^{2\pi i sq_0^{(j)}(t - sq_0^{(j)}) \cot \theta} \Phi_j(t - sq_0^{(j)})$ .  $\Psi_\theta$  presents a redundant set of basis functions that can be used to represent or analyze a signal on the fractional domain. Unlike FrFT, it is equipped with adaptive windows  $\Psi_j$  over each scale  $j$  to capture a wide range of signal behaviors. Building upon this, we propose fractional neural frame operator.

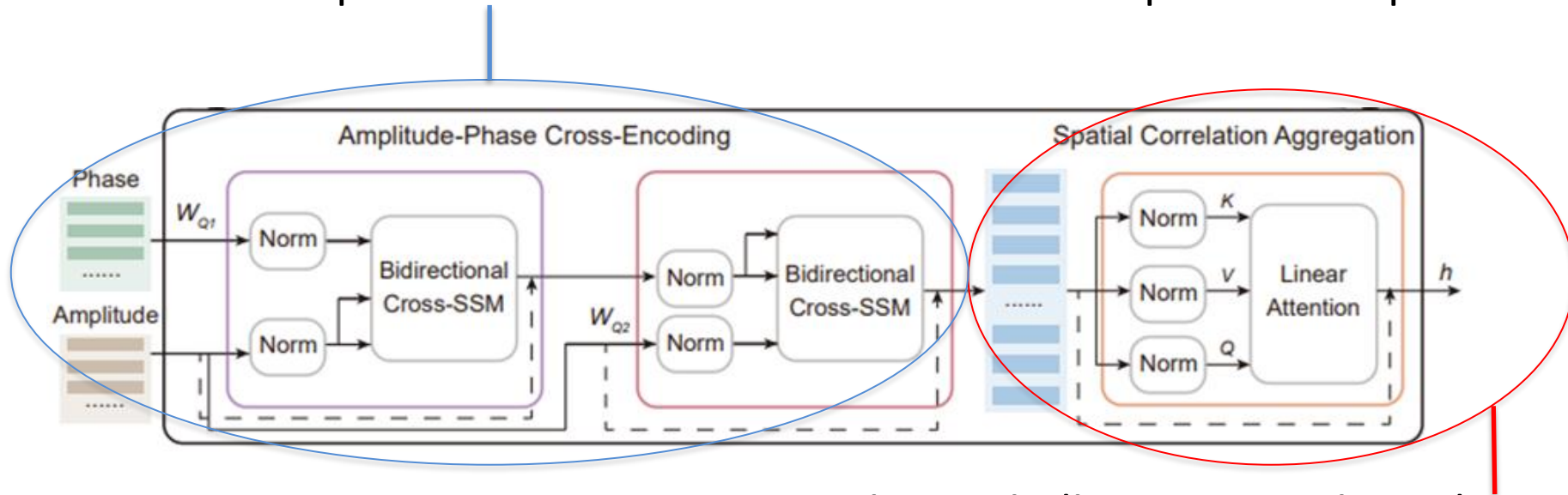
The core of the FrNFO is an implicit multilayer perceptron (MLP) [37, 66] designed to generate adaptive window function for the frame filters. Given temporal samples  $N$  and feature channels  $d_{\text{model}}$ , the implicit MLP defines the window kernel  $\Phi \in \mathbb{C}^{N \times d_{\text{model}}}$  for  $j = 1, \dots, N$ ,  $k = 1, \dots, d_{\text{model}}$  as

$$\Phi^{j,k}(t_j) = \left( \sum_{i=1}^M w_{i,k} \exp(-j(b_{i,k}t_j + c_{i,k})) \right) \cdot \left( \sum_{n=0}^K a_{n,k} H_n(t_j) \right), \quad (4)$$

where  $w_{i,k}, b_{i,k}, c_{i,k}, a_{n,k}$  are trainable parameters optimized through gradient descent. The basis functions  $H_n(t) = (-1)^n e^{t^2} \frac{d^n}{dt^n} e^{-t^2}$  are Hermite polynomials, embedding prior knowledge of localized oscillatory behavior, while the sine activation functions promote smooth and periodic kernel characteristics essential for identifying quasiperiodic activities in brain.

# APCE & SCA

- Dual bidirectional selective state-space (BSSM) modules.
- Phase-to-Amplitude and Amplitude-to-Phase interactions.
- Dynamic transitions conditioned by complementary embeddings.
- Residual fusion captures mutual information between amplitude and phase.



- Linear attention across channels (linear complexity).
- 3×3 depthwise convolution + RMSNorm aggregates local patterns.
- Sigmoid gating improves robustness and stability.

# Datasets

- 12 Benchmarks Across Humans, Dogs, Rats, & Macaques
- Modalities: Scalp-EEG, SEEG, ECoG, LFP, Standardized 64-Channel Inputs for Fair
- Reveals shared pre-seizure signals (e.g., SASP) across species, from rodents to primates—challenges "epilepsy is uniquely individual" myth.

Dataset	Confidentiality	Species	# Subj.	Modality	# Ch.	# Samples	Duration	SOP	SPH	ID/IV	OOD/EV
FMCE	Public	Human	65	ECoG/SEEG <sup>1</sup>	64	32,323	4 s	30 s	1 min	✓	✗
HUP	Public	Human	73	ECoG/SEEG	64	53,323	4 s	30 s	5 min	✓	✗
RESPECT	Public	Human	6	ECoG	64	17,214	4 s	30 s	5 min	✓	✗
BEIRUT	Public	Human	6	Scalp-EEG	64	35,941	4 s	1 min	30 min	✓	✓
CTLE-RATLFP	Public	Rat	7	LFP	64	11,732	2 s	30 s	5 min	✓	✗
LPIRE	Public	Rat	15	LFP	64	159,715	2 s	30 s	5 min	✓	✓
CANINE	Public	Dog	6	ECoG	64	382,278	4 s	5 min	4 hr	✓	✓
ATLE	Private	Human	5	Scalp-EEG	64	11,536	4 s	5 min	30 min	✓	✗
AGS	Private	Human	5	Scalp-EEG	64	32,323	4 s	5 min	30 min	✓	✓
IESS	Private	Human	17	Scalp-EEG	64	48,986	4 s	5 min	30 min	✓	✓
KAIME	Private	Macaque	3	Scalp-EEG & SEEG <sup>2</sup>	64	36,092	4 s	5 min	30 min	✓	✓
PCS	Private	Human	5	Scalp-EEG	64	29,679	4 s	5 min	30 min	✓	✗
TUEG	Public	Human	14,987	Scalp-EEG	64	1,030,090	32 s	Used for Pretraining Only			
CCEP	Public	Human	74	ECoG	64	52,337	32 s	Used for Pretraining Only			
PPE	Public	Human	30	Scalp-EEG	64	13,434	32 s	Used for Pretraining Only			

<sup>1</sup> For “ECoG/SEEG” datasets each subject has *either* sub-dural ECoG grids/strips *or* SEEG depth electrodes, never both.

<sup>2</sup> KAIME comprises simultaneous scalp-EEG and SEEG depth recordings from three adult rhesus macaques (*Macaca mulatta*).

# Main Results

- Evaluated on **7 public benchmarks**: BEIRUT, CANINE, FMCE, CTLE-RATLFP, LPIRE, HUP, and RESPECT.
- **FAPEX-Base** achieves **Top-1 F1 and Sensitivity** on all 7 datasets; **Top-1 ROC** on 6/7.
- Outperforms supervised baselines such as **TimeMixer**, **Medformer**, **EEGConformer**, and **PatchTST** by **≈10–15%** in Sensitivity.
- Compared to self-supervised baselines (**CBraMod**, **Neuro-BERT**, **VQ\_MTM**), **FAPEX-Base (SSL)** gains an additional **3–5%** in F1 and AUROC.
- These results demonstrate robust generalization across **species** (human, rat, dog) and **modalities** (EEG, ECoG, SEEG, LFP).

**Table 2: Median performance across publicly available datasets.** **Top-1**, **Top-2**, and **Top-3** results are highlighted in red, blue, and green, respectively, within both supervised (SL) and self-supervised (SSL) groups. **FAPEX** demonstrates consistently strong performance, achieving top-1 TO 3 rankings on the majority of datasets and metrics, reflecting its generalization and adaptability. For detailed results and statistical analysis, refer to App. C.

Model	BEIRUT			CANINE			FMCE			CTLE-RATLFP			LPIRE			HUP			RESPECT		
	SEN	F1	ROC	SEN	F1	ROC	SEN	F1	ROC	SEN	F1	ROC	SEN	F1	ROC	SEN	F1	ROC	SEN	F1	ROC
ModernTCN	83.4	83.1	85.0	84.8	84.0	73.4	79.6	89.3	88.7	69.2	74.0	89.5	68.7	72.6	80.3	71.3	70.3	67.3	70.0	75.0	80.0
MIRConv	78.6	78.2	83.5	83.7	83.8	72.6	78.8	89.9	88.2	73.0	76.4	73.0	60.5	68.4	68.7	69.1	67.8	66.1	71.1	72.7	73.8
MultiresNet	73.3	72.8	74.7	64.8	72.0	70.8	75.8	82.5	83.3	63.0	68.8	87.1	67.1	71.7	80.1	65.3	63.8	65.5	62.4	75.2	61.7
Omni-Scale	72.6	71.5	83.1	65.3	71.9	73.2	79.1	84.1	83.7	75.8	78.3	72.5	51.9	65.1	75.7	70.7	68.7	67.1	69.2	73.3	75.7
SPaRCNet	71.1	71.6	79.1	85.9	84.7	74.0	60.4	67.7	65.9	72.2	75.5	67.5	43.6	48.2	50.8	61.6	60.2	62.8	73.7	81.3	63.0
EEGConformer	68.4	66.5	82.5	79.3	81.4	52.9	73.0	85.0	81.4	73.5	76.8	72.3	58.5	65.8	70.2	64.6	63.3	64.6	82.5	84.6	86.5
EEGMamba	70.0	68.5	82.6	79.6	81.2	53.2	68.9	95.5	85.7	62.0	68.0	89.5	63.7	70.7	80.7	63.2	61.3	62.8	79.6	80.0	73.0
iTransformer	70.6	69.2	82.8	64.2	70.4	71.2	68.4	80.0	78.3	56.2	62.6	75.6	40.9	46.0	49.4	58.3	57.7	57.4	80.5	84.7	87.9
Nonformer	68.6	63.4	75.2	60.7	64.9	70.3	74.9	82.6	86.5	72.6	76.3	80.9	64.2	74.4	76.1	62.1	61.9	62.4	74.1	78.7	81.6
PatchTST	71.9	72.5	79.3	77.6	80.6	72.8	74.2	91.8	86.6	73.3	76.5	72.0	50.2	50.4	52.6	70.8	69.3	67.5	86.5	86.9	82.2
Pathformer	67.6	64.1	81.7	65.9	72.3	71.8	77.9	91.2	88.9	80.4	81.3	82.8	68.7	73.0	80.1	65.7	65.2	66.3	76.9	79.9	82.7
SeizureFormer	67.0	60.2	79.8	78.8	81.8	53.5	73.6	78.8	79.3	56.6	63.0	84.5	65.6	73.2	68.2	59.7	59.4	61.0	83.1	85.0	74.3
ATFNet	76.0	74.6	79.4	62.8	70.9	71.3	73.4	81.3	82.7	54.1	60.7	78.2	40.0	44.9	50.0	64.5	60.4	63.6	78.4	82.9	85.7
FreTS	64.7	58.6	81.8	46.8	54.3	69.5	62.0	68.3	61.4	49.2	56.5	68.5	34.9	38.6	49.4	62.6	50.1	57.2	64.0	72.5	78.4
NFM	77.3	75.7	79.7	71.5	76.9	72.0	74.4	91.8	86.4	46.5	52.5	74.0	37.3	43.0	48.8	62.7	63.4	64.4	75.0	77.0	80.8
TSLANet	83.4	83.1	85.0	85.7	84.4	73.0	74.2	91.8	86.6	65.3	70.7	88.9	68.6	72.2	79.9	67.9	66.5	67.5	74.3	78.7	76.2
AdaWaveNet	68.0	66.1	82.7	79.8	81.3	52.9	76.6	82.6	87.3	55.2	61.4	83.6	54.1	66.2	76.2	64.0	63.2	64.4	78.2	84.1	66.6
Medformer	83.8	83.1	84.4	85.9	84.5	74.1	77.8	83.6	88.6	70.0	74.3	86.7	66.7	72.3	80.6	64.8	64.3	65.0	59.7	68.0	70.5
MTST	80.3	78.4	84.1	68.0	74.5	72.5	75.5	89.3	87.7	70.8	74.7	69.5	45.3	49.6	50.4	65.9	64.4	66.2	79.4	82.9	82.2
Pyraformer	82.8	81.7	85.4	80.8	82.3	72.7	67.0	96.3	79.8	60.9	66.9	86.5	60.2	72.1	76.2	60.5	58.2	58.9	64.0	72.5	78.4
SimpleTM	82.6	82.0	83.4	82.8	83.3	72.5	74.4	80.5	80.6	72.5	76.0	70.9	47.5	52.0	51.1	67.8	65.2	68.5	74.5	77.7	70.0
TimesNet	70.3	70.6	78.4	67.3	74.1	72.3	67.0	74.6	73.4	63.4	69.0	74.2	47.1	49.4	51.5	65.9	61.7	65.4	64.2	63.4	76.9
TimeMixer	71.8	72.3	79.0	76.6	80.0	73.0	78.8	82.9	84.5	69.0	73.8	87.9	66.2	72.0	80.6	67.1	66.2	67.3	72.1	76.5	81.9
FAPEX-Small (SL)	83.9	83.8	85.2	85.8	84.7	74.2	87.4	90.6	97.0	76.9	80.2	89.9	69.3	73.4	81.2	72.6	72.0	78.3	86.2	87.1	89.3
FAPEX-Base (SL)	84.7	84.3	85.8	86.0	84.7	74.5	88.8	90.7	97.2	81.8	83.2	91.2	71.7	76.1	81.0	73.7	72.5	79.3	92.3	92.3	91.6
Brant	71.0	71.7	78.9	93.2	92.7	96.6	75.2	74.7	86.8	72.1	76.3	83.6	56.8	68.6	75.8	64.0	63.2	63.9	70.6	70.4	76.0
CBraMod	83.9	83.5	85.5	90.8	90.6	98.7	79.2	79.9	88.8	82.0	81.9	82.8	69.3	74.9	68.4	56.5	54.4	79.6	62.1	69.5	67.6
EEGPT	63.9	73.3	71.9	93.4	92.9	98.5	68.8	68.9	74.7	58.7	64.6	86.2	65.1	71.5	80.5	61.3	58.8	58.8	76.8	82.2	60.4
Neuro-BERT	85.4	85.2	86.9	93.7	93.2	96.8	77.9	78.1	87.7	72.7	76.8	85.5	68.6	73.8	81.5	56.5	54.4	79.6	67.3	74.6	82.4
VQ_MTM	74.5	75.0	82.7	87.9	85.5	94.6	73.7	74.3	82.3	72.6	75.8	69.7	50.7	55.5	63.7	62.1	63.5	64.9	66.8	67.3	81.7
COMETS	86.2	86.0	87.3	93.9	93.4	98.2	76.1	76.3	87.1	74.2	77.4	83.7	53.4	61.6	68.6	65.2	64.1	66.4	76.3	81.5	75.6
MF-CLR	78.2	76.5	83.8	91.2	90.0	97.0	79.5	80.1	88.5	66.6	71.8	88.5	47.6	51.3	50.6	67.1	66.2	67.3	76.3	82.2	76.8
TS2Vec	57.1	67.0	58.7	94.7	94.5	97.5	75.5	74.5	87.7	72.0	75.3	77.8	59.7	64.1	51.8	58.9	51.6	56.7	79.6	82.6	78.5
FAPEX-Small	87.5	86.7	90.0	94.1	93.7	98.4	89.5	89.6	97.5	84.8	86.2	90.4	72.0	75.8	81.2	72.0	72.1	79.4	79.0	82.3	89.8
FAPEX-Base	87.8	87.3	89.9	95.2	94.9	99.7	91.5	91.5	98.0	85.2	86.5	90.6	78.9	83.7	75.2	77.1	77.2	81.1	93.1	94.6	95.2



# Main Results

**Table 3: Median Performance Across In-House Datasets.** Top-1, Top-2, and Top-3 results are highlighted in red, blue, and green, respectively, within both supervised (SL) and self-supervised (SSL) groups. **FAPEX** demonstrates consistently strong performance, achieving top-1 TO 3 rankings on the majority of datasets and metrics, reflecting its generalization and adaptability. For detailed results and statistical analysis, refer to App. C.

Model	AGS			ATLE			IESS			KAIME			PCS		
	SEN	F1	ROC	SEN	F1	ROC	SEN	F1	ROC	SEN	F1	ROC	SEN	F1	ROC
ModernTCN	87.0	85.0	93.2	91.7	90.2	100.0	73.4	73.4	67.2	83.4	73.2	87.3	85.9	85.4	86.3
MRConv	91.3	90.3	95.2	86.6	96.1	100.0	68.8	68.7	66.9	81.1	68.5	85.0	83.0	84.1	83.7
MultiresNet	90.1	88.8	96.1	85.4	84.3	100.0	72.1	70.4	68.7	80.4	63.7	82.5	69.2	64.4	83.9
Omni-Scale	91.7	90.9	95.2	87.8	98.6	99.9	67.9	68.7	67.2	81.0	68.8	83.0	80.0	79.6	80.9
SPaRCNet	89.1	87.5	93.4	84.0	81.7	99.8	60.7	64.9	61.4	82.0	77.1	86.5	85.5	84.4	91.0
EEGConformer	89.8	88.5	94.4	88.5	91.2	100.0	66.1	67.9	67.0	81.4	73.4	87.1	77.1	78.8	84.3
EEGMamba	93.8	93.5	96.8	88.2	85.0	100.0	69.6	70.0	68.8	80.4	69.4	83.4	70.8	73.3	85.6
iTransformer	89.5	87.8	95.3	54.9	2.9	99.8	53.4	54.5	66.4	81.3	63.4	87.1	74.3	73.0	83.4
Nonformer	93.2	92.7	96.7	84.7	97.5	99.8	69.7	74.7	68.9	79.5	90.3	81.6	68.8	63.7	84.1
PatchTST	90.5	89.3	95.5	86.6	93.0	100.0	61.6	63.8	67.5	83.0	73.8	88.5	71.9	71.2	73.8
Pathformer	92.5	91.8	96.7	88.7	95.3	100.0	71.3	72.1	68.6	80.6	67.4	85.3	78.7	80.9	83.7
SeizureFormer	92.1	91.3	95.4	86.3	97.9	99.9	69.7	69.9	66.7	77.3	53.4	85.9	58.6	62.4	59.7
ATFNet	85.2	84.1	90.8	83.1	97.0	99.8	59.7	56.2	68.2	65.0	45.7	71.9	74.7	73.5	84.6
FreTS	88.7	87.0	93.0	70.2	70.8	77.8	42.7	32.8	67.0	54.3	56.4	73.8	70.5	72.7	77.8
NFM	88.7	87.0	93.0	71.3	71.8	81.7	52.4	56.2	61.2	76.8	64.4	80.4	73.6	76.9	83.0
TSLANet	94.4	94.2	97.3	91.4	91.6	100.0	73.8	72.9	66.2	82.2	88.4	82.4	84.6	84.0	84.9
AdaWaveNet	89.0	87.6	95.1	82.8	96.6	99.8	70.0	70.7	66.3	70.5	77.7	84.8	72.4	74.2	81.3
Medformer	88.7	88.0	96.1	88.2	98.9	99.9	73.7	73.1	66.9	73.2	45.2	72.3	77.9	77.1	96.3
MTST	91.6	90.7	98.0	84.1	97.2	99.8	60.3	56.4	70.1	59.0	60.2	74.2	72.8	70.3	74.1
Pyraformer	92.0	91.3	96.5	85.1	97.7	99.8	71.4	70.2	66.9	83.2	56.6	86.4	76.8	79.9	82.3
SimpleTM	85.1	83.5	88.2	90.8	90.4	99.9	66.7	68.8	64.4	80.0	81.1	84.6	76.0	75.0	84.5
TimesNet	89.7	88.3	94.3	82.1	96.3	99.8	59.9	63.6	66.1	80.0	81.1	84.6	77.7	81.0	84.6
TimeMixer	92.3	91.6	96.6	87.9	95.3	100.0	71.7	71.0	68.6	82.1	90.0	85.2	81.1	83.5	85.4
FAPEX-Small (SL)	94.1	93.7	98.4	87.2	98.4	99.9	70.8	70.4	71.7	86.9	92.1	89.3	81.0	81.2	94.1
FAPEX-Base (SL)	94.9	94.6	99.5	88.0	98.8	99.9	72.3	72.4	71.4	87.0	95.6	90.1	91.5	91.5	96.3
Brant	93.2	92.7	96.6	87.9	83.0	99.9	68.0	67.7	69.5	74.5	74.8	74.4	83.1	82.3	95.8
CBraMod	90.8	90.6	98.7	87.9	82.8	99.9	79.6	80.7	76.2	81.0	79.8	83.7	81.1	83.5	85.4
EEGPT	93.4	92.9	98.5	88.2	83.2	100.0	74.2	73.9	71.4	78.4	77.3	78.6	85.5	84.4	91.0
Neuro-BERT	93.7	93.2	96.8	83.3	90.8	100.0	75.3	75.0	71.5	81.7	80.7	83.6	80.8	81.9	96.8
VQ_MTM	87.9	85.5	94.6	81.7	79.5	99.9	72.8	72.9	69.8	62.8	64.7	78.2	81.0	81.2	94.1
COMETS	93.9	93.4	98.2	87.7	83.2	99.8	67.6	68.2	79.3	80.6	80.1	84.0	80.8	81.9	96.8
MF-CLR	91.2	90.0	97.0	84.4	82.8	100.0	79.7	80.8	75.6	80.9	79.8	86.3	79.2	77.4	97.2
TS2Vec	94.7	94.5	97.5	62.7	76.1	73.6	72.4	73.6	72.9	76.1	76.2	76.7	69.0	65.9	96.4
FAPEX-Small (SSL)	94.1	93.7	98.4	94.0	92.8	100.0	81.5	83.7	83.4	87.4	87.1	89.3	91.0	91.0	96.7
FAPEX-Base (SSL)	95.2	94.9	99.7	94.8	98.0	100.0	83.7	84.9	85.9	88.7	88.4	91.4	95.0	95.0	97.5

- Evaluated on **5 private datasets**: AGS, ATLE, IESS, KAIME, and PCS.
- FAPEX-Base (SL)** surpasses all baselines in both **F1** and **Sensitivity**, often exceeding **95% ROC**.
- On IESS and KAIME, FAPEX-Base (SSL) reaches **>98% ROC** and **>94% F1**, indicating strong within-institution consistency.
- Self-supervised pretraining further improves low-data robustness — especially in **ATLE** and **KAIME**, where labeled data are scarce.
- The architecture scales effectively across different EEG configurations and species (**human, macaque**) without retraining from scratch.

# Cross-Cohort Transfer & Generaliza

- Tested in source-only, domain generalization, semi-supervised, and domain adaptation setups.
- Consistent F1 gains (>30%) even without target labels.
- Robust across species, institutions, and modalities.

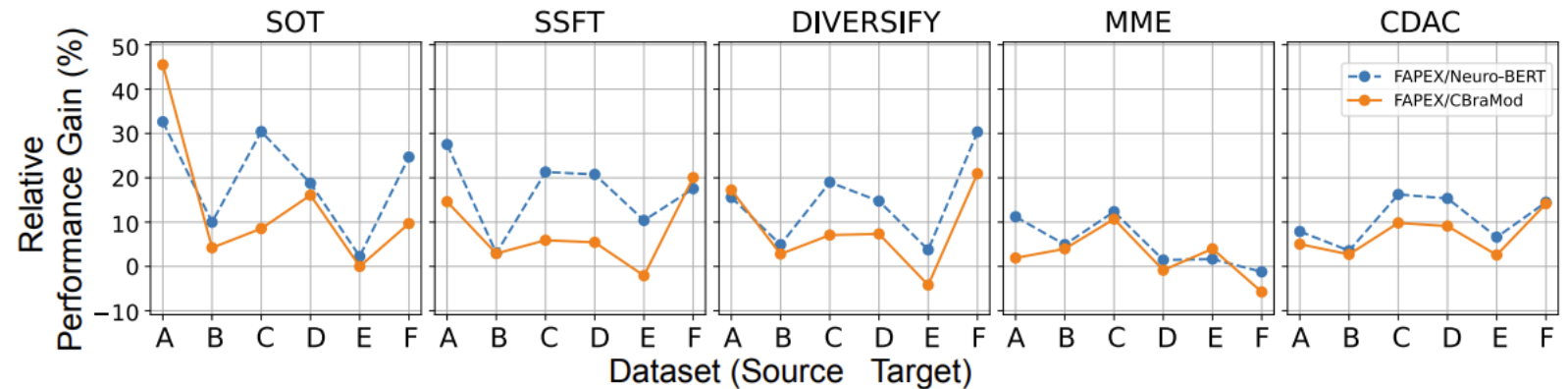


**Figure 4: Relative improvement in F1-score medians ( $\Delta\%$ ) of FAPEX-Base over **Neuro-BERT** and **CBraMod** across five distinct transfer learning setups for six source-target dataset pairs.** FAPEX-Base demonstrates consistent performance gains for most cases, under both weak (SOT) and stronger supervision regimes (CDAC). A: KAIME  $\rightarrow$  AGS, B: AGS  $\rightarrow$  BEIRUT, C: IESS  $\rightarrow$  BEIRUT, D: LPIRE  $\rightarrow$  AGS, E: LPIRE  $\rightarrow$  IESS, F: LPIRE  $\rightarrow$  KAIME). FAPEX-Base consistently achieves superior performance.

# Conclusions

- Achieved **Top-1 results on 12 datasets** spanning **four species** and **multiple EEG modalities**.
- Demonstrated **consistent superiority** over 30+ supervised and self-supervised baselines.
- Provided **evidence of a distinct preictal state**, confirming the existence of predictable neural dynamics before seizures.

**Future Directions:** *Data Expansion, Multimodal Integration, Edge & Wearable Deployment, etc..*

# Acknowledgements



This work was supported by the Science and Technology Innovation 2030 - Brain Science and BrainInspired Intelligence Project (Grant No. 2021ZD0201301), the National Natural Science Foundation of China (Grant Nos. 9257020, U20A20221, 12147101), and the Shanghai Municipal Science and Technology Committee of Shanghai Outstanding Academic Leaders Plan (Grant No. 21XD1400400). We thank the Shanghai Institute for Mathematics and Interdisciplinary Sciences (SIMIS) for financial support (Grant No. SIMIS-ID-2025-NC). The computations were performed on the CFFF platform of Fudan University.